Effect of chiral nuclear forces on the neutrino mean free path in hot neutron matter

Isaac Vidaña,[1] Domenico Logoteta,[2,3] and Ignazio Bombaci[2,3]
[1]*Istituto Nazionale di Fisica Nucleare, Sezione di Catania, Dipartimento di Fisica e Astronomia "Ettore Majorana", Università di Catania, Via Santa Sofia 64, I-95123 Catania, Italy*
[2]*Dipartimento di Fisica "Enrico Fermi", Università di Pisa, Largo B. Pontecorvo 3, I-56127 Pisa, Italy*
[3]*Istituto Nazionale di Fisica Nucleare, Sezione di Pisa, Largo B. Pontecorvo 3, I-56127 Pisa, Italy*

(Received 22 June 2022; revised 11 August 2022; accepted 7 September 2022; published 16 September 2022)

We study the role of chiral nuclear forces on the propagation of neutrinos in hot neutron matter. In particular, we analyze the convergence of the dynamical structure factor and the neutrino mean free path with the order of the power counting of the chiral forces, as well as the role of the regulator cutoff of these forces in the determination of these quantities. Single-particle energies and chemical potentials needed to calculate the dynamical structure factor are obtained within the Brueckner-Hartree-Fock approximation extended to finite temperature. Our results show that the dynamical structure factor and the neutrino mean free path depend on the cutoff only when the chiral potential is considered at leading order (LO) and next-to-leading order (NLO), with this dependence becoming strongly reduced at higher orders in the chiral power counting due to the role of three-nucleon forces that start to contribute at next-to-next-to-leading order (N^2LO) and being, in particular, almost negligible at next-to-next-to-next-to-leading order (N^3LO). The neutrino mean free path is found to converge up to densities slightly below ≈ 0.15 fm^{-3} when increasing the order of the chiral power counting, although no signal of convergence is found for densities above this value. The uncertainty associated with our order-by-order nuclear many-body calculation of the neutrino mean free path is roughly estimated from the difference between the results obtained at N^2LO and N^3LO, finding that it varies from about a few centimeters at low densities up to a bit less than 2 m at the largest one considered in this work, 0.3 fm^{-3}.

DOI: 10.1103/PhysRevC.106.035804

I. INTRODUCTION

Neutrinos and, particularly, the knowledge of their interactions in hot and dense baryonic matter [1–50] are fundamental to understand the physics of supernova explosions [51–53] and the early evolution of their compact stellar remnants [54,55]. The gravitational collapse of massive stars at the end of their thermonuclear burning leads, by means of electron capture processes, to the production of a large number of neutrinos which store and release most of the initial gravitational binding energy. In the early stages following the formation of neutron stars neutrinos are trapped because, above a critical value of the density, their mean free path λ decreases and becomes much smaller than the stellar radius. This trapping has a strong influence on the composition and on the overall stiffness of the equation of state (EoS) of neutron stars [56–59], with the physical conditions of hot and lepton-rich neutron stars being in general substantially different from those of cold and deleptonized ones. In particular, neutrino trapping keeps the concentration of electrons so high that matter is more proton rich in comparison with the case in which neutrinos have diffused out. Neutrinos are also very important to understand the merger [60–64] and the cooling [65–67] of neutron stars. Cooling is driven first by neutrino emission mechanisms such as direct and modified Urca processes, bremsstrahlung, and Cooper pair formation, the last operating only when the temperature of the star drops below the critical temperature for neutron superfluidity or proton superconductivity. Numerical simulations of supernova explosions and neutron star mergers, as well as cooling calculations, require not only the knowledge of the hot dense matter EoS but also a reliable description of neutrino transport. Whereas the most detailed transport codes, which solve the full Boltzmann transport equation, require the knowledge of neutrino differential cross sections, simpler transport codes only need angle averaged and/or energy averaged neutrino opacities, usually expressed in the form of neutrino mean free paths. Important sources of neutrino opacities are neutrino-baryon scattering and neutrino-baryon absorption reactions mediated, respectively, by the neutral current and the charge current of the electroweak interaction. The interested reader is referred to Refs. [68–71] for recent progress in the study of neutrino opacities in hot and dense nuclear matter.

In this work we consider the propagation of neutrinos in hot neutron matter and, therefore, we take into account only the contribution of the scattering of neutrinos off neutrons in the evaluation of the neutrino mean free path. The extension of the present study to the case of hot asymmetric nuclear matter, more relevant to describe the physical conditions of newly born neutron stars, will be considered in the near future [72]. Here, in particular, we study the effect of chiral nuclear forces on the neutrino mean free path, our main focus being

the analysis of the convergence of the dynamical structure factor and the neutrino mean free path with the order of the power counting of the chiral forces when going from the leading order (LO) to the next-to-next-to-next-to-leading order (N^3LO), as well as the role played by the cutoff of these forces in the determination of these quantities. A microscopic framework based on an extension to finite temperature of the Brueckner-Hartree-Fock (BHF) approximation of the Brueckner-Bethe-Goldstone (BBG) theory is employed to describe in a consistent way both the EoS of pure neutron matter and the dynamical structure factor. Whereas, in the past years, nuclear forces derived within the framework of chiral effective field theory (χEFT) have been largely used to determine the nuclear EoS within different many-body techniques [73–87], less attention has been paid to the role played by these forces in calculations of neutrino processes in dense matter (see, e.g., Refs. [88–91]).

The paper is organized in the following way. The neutrino-neutron scattering cross section is briefly reviewed in Sec. II. The role of chiral forces in the dynamical structure factor and neutrino mean free path is analyzed in Sec. III. Finally, a summary and the main conclusions of this work are drawn in Sec. IV.

II. NEUTRINO-NEUTRON SCATTERING CROSS SECTION

In this section we briefly review the expression for the neutrino-neutron cross section scattering in hot neutron matter. Using the Fermi golden rule (see, e.g., Ref. [92]) the cross section per unit volume (or equivalently the inverse collision mean free path) for the scattering process, which is mediated by the neutral current of the electroweak interaction, can be written as

$$\frac{\sigma(E_\nu,T)}{V}=2\int\frac{d^3\vec{p}_{\nu'}}{(2\pi)^3}\int\frac{d^3\vec{p}_n}{(2\pi)^3}\int\frac{d^3\vec{p}_{n'}}{(2\pi)^3}(2\pi)^4\delta^4(p_\nu+p_n-p_{\nu'}-p_{n'})(1-f_{\nu'}(E_{\nu'},T))f_n(E_n,T)(1-f_{n'}(E_{n'},T))\times\frac{\langle|\mathcal{M}|^2\rangle}{16E_1E_2E_3E_4},\tag{1}$$

where the invariant transition matrix $\mathcal{M}$ reads

$$\mathcal{M}=\frac{G_F}{2\sqrt{2}}(\bar{\psi}_{\nu'}\gamma^\mu(1-\gamma_5)\psi_\nu)(\bar{\psi}_{n'}\gamma_\mu(C_V-C_A\gamma_5)\psi_n),\tag{2}$$

with $G_F\simeq 1.436\times10^{-49}$ erg cm^{-1} being the Fermi weak coupling constant, and $C_V=-1$ and $C_A=-1.23$ the vector and axial-vector couplings. The symbol $\langle\cdot\rangle$ denotes a sum over final spins and an average over the initial ones, $p_i=(E_i,\vec{p}_i)$ is the four-momentum of particle i, and $f_i(E_i,T)$ is its Fermi-Dirac distribution,

$$f_i(E_i,T)=\frac{1}{1+\exp[(E_i(T)-\mu_i(T))/T}},\tag{3}$$

where E_i and μ_i are, respectively, the single-particle energy and chemical potential of the corresponding particle. The neutron single-particle energy and chemical potential are obtained, as it is explained below, from an extension to finite temperature of the nonrelativistic BHF approximation using nuclear forces derived within the framework of χEFT.

In the limit of nonrelativistic neutrons and nondegenerate neutrinos, the scattering cross section simplifies and reads [9]

$$\frac{\sigma(E_\nu,T)}{V}=\frac{G_F^2}{32\pi^2}\int d^3\vec{p}_{\nu'}\big[C_V^2(1+\cos\theta_{\nu\nu'})S^{(0)}(q_0,\vec{q},T)+C_A^2(3-\cos\theta_{\nu\nu'})S^{(1)}(q_0,\vec{q},T)\big],\tag{4}$$

where $q=p_\nu-p_{\nu'}$ is the transferred four-momentum from the neutrino to the neutron system, $\theta_{\nu\nu'}$ is the angle between the incoming and outgoing neutrino, and $S^{(S)}(q_0,\vec{q},T)$ is the dynamical structure factor that describes the response of neutron matter in the spin channel $S=0,1$ to the excitations induced by neutrinos, and contains the relevant information of the nuclear medium. The vector and axial parts of the neutral current give rise, respectively, to density and spin-density fluctuations, corresponding to the $S=0$ and $S=1$ spin channels. The dynamical structure factor can be obtained from the imaginary part of the corresponding response function $\chi^{(S)}(q_0,\vec{q},T)$ via the fluctuation-dissipation theorem [93],

$$S^{(S)}(q_0,\vec{q},T)=-\frac{g}{\pi}\frac{1}{1-\exp[-q_0/T]}\mathrm{Im}\,\chi^{(S)}(q_0,\vec{q},T),\tag{5}$$

where $g=2$ is the spin degeneracy of the neutrons and the factor $(1-\exp[-q_0/T])^{-1}$ has the appearance of a step function except around $q_0=0$ where it diverges as $1/q_0$. However, the dynamical structure factor does not show any divergency because the imaginary part of the response function behaves as q_0 around $q_0=0$. The response function can be obtained from the bare one $\chi_0(q_0,\vec{q},T)$ and the particle-hole residual interaction $V_{ph}^{(S)}(q_0,\vec{q})$ within the random phase approximation (RPA) by solving the integral equation

$$\chi^{(S)}(q_0,\vec{q},T)=\frac{\chi_0(q_0,\vec{q},T)}{1-V_{ph}^{(S)}(q_0,\vec{q})\chi_0(q_0,\vec{q},T)}.\tag{6}$$

In this work, however, we ignore the role played by the long-range correlations induced from the particle-hole residual interaction (i.e., we take $V_{ph}^{(S)}(q_0,\vec{q})=0$) and, then, we simply assume $\chi^{(S)}(q_0,\vec{q},T)=\chi_0(q_0,\vec{q},T)$, independently of the spin channel. Therefore, from now on, we will omit the spin index in the dynamical structure factor. Nonetheless, interactions among neutrons are taken into account at the mean field level in the calculation of $\chi_0(q_0,\vec{q},T)$:

$$\chi_0(q_0,\vec{q},T)=\int\frac{d^3\vec{p}}{(2\pi)^3}\frac{f_n(E_n(\vec{p},T),T)-f_n(E_n(\vec{p}+\vec{q},T),T)}{q_0-E_n(\vec{p}+\vec{q},T)+E_n(\vec{q},T)+i\eta}.\tag{7}$$

The neutron single-particle energy and chemical potential needed to calculate $\chi_0(q_0, \vec{q}, T)$ are obtained, as mentioned before, from an extension to finite temperature of the nonrelativistic BHF approximation with chiral forces. This extension basically consists of replacing the zero temperature neutron occupation number

$$n(\vec{k}) = \begin{cases} 1 & \text{if } |\vec{k}| \leqslant k_F \\ 0 & \text{otherwise} \end{cases} \tag{8}$$

by the corresponding Fermi-Dirac momentum distribution when calculating the BHF single-particle energy,

$$E_n(\vec{k}, T) = \frac{\hbar^2 k^2}{2m} + \mathrm{Re}\, U_n(\vec{k}, T). \tag{9}$$

Here $U_n(\vec{k}, T)$ is the neutron single-particle potential given at finite temperature by

$$U_n(\vec{k}, T) = \sum_{\vec{k}'} f_n(E_n(\vec{k}', T), T) \times \langle \vec{k}\vec{k}' | G(E_n(\vec{k}, T) + E_n(\vec{k}', T), T) | \vec{k}\vec{k}' \rangle_{\mathcal{A}}, \tag{10}$$

where the G matrix, describing the effective interaction between two neutrons in the presence of a surrounding medium, is obtained by solving the Bethe-Goldstone equation which at finite temperature reads schematically

$$G(\omega, T) = V + \sum_{ij} V \frac{(1 - f_n(E_n(\vec{k}_i, T), T)(1 - f_n(E_n(\vec{k}_j, T), T)}{\omega - E_n(\vec{k}_i, T) - E_n(\vec{k}_j, T) + i\eta} G(\omega, T). \tag{11}$$

Here V is the bare nucleon-nucleon interaction of which we give some details at the end of this section, and ω is the sum of the nonrelativistic single-particle energies of the interacting neutrons.

We note that the self-consistent solution of Eqs. (9)–(11) requires to extract the neutron chemical potential at each step of the iterative process from the normalization condition

$$\rho = \sum_{\vec{k}} f_n(E_n(\vec{k}, T), T), \tag{12}$$

with ρ being the neutron density.

Before finishing this section we would like to say a few words on the nuclear forces employed in this work. As already said, we make use of nuclear forces derived within the framework of χEFT. In particular, we use the chiral nuclear force of Entem and Machleidt [94] up to N^{3}LO and consider three values of the cutoff Λ, 450, 500, and 550 MeV. The contribution from three-nucleon forces to the neutron single-particle potentials and consequently to the dynamical structure factor and the neutrino mean free path, which appear at N^{2}LO and higher orders [95,96], is introduced in our BHF calculation by averaging over the coordinates of one of the neutrons. This leads to an effective density dependent two-body force which is added to the two-body one before solving the Bethe-Goldstone equation. The interested reader can find explicit expressions for this effective density dependent two-body force, e.g., in Refs. [97–99].

In the next section we analyze the role of the cutoff dependence of the forces on the determination of the dynamical structure factor and the neutrino mean free path as well as the convergence of these quantities when considering different orders in the power counting of the chiral nuclear forces from LO up to N^{3}LO.

III. DYNAMICAL STRUCTURE FACTOR AND NEUTRINO MEAN FREE PATH

We start this section by showing in Fig. 1 the dynamical structure factor $S(q_0, \vec{q}, T)$ as a function of the transferred energy q_0 for several temperatures at a fixed value of the density $\rho = 0.16$ fm^{-3} [Fig. 1(a)] and various densities for $T = 10$ MeV [Fig. 1(b)]. The calculation is done using the chiral potential at N^{3}LO including two- and three-nucleon forces with a cutoff $\Lambda = 500$ MeV. The three-momentum transferred is fixed to the value $|\vec{q}| = 15$ MeV. In this figure and all the rest, the energy of the neutrino is assumed to be $E_\nu = 3T$. As it can be seen in the figure, an increase of the temperature or the density leads to a much broader dynamical structure factor with a larger area under it. The reason is simply due to the fact that the phase space of the integral in Eq. (7) increases with the temperature and the density. Consequently, an increase of the temperature or the density will give rise to a larger cross section and, therefore, to a smaller neutrino mean free path λ when integrating Eq. (4). This is seen in Fig. 2, where λ is shown as a function of the baryon number density for several temperatures. We notice that the range of densities under consideration is such that the Fermi momentum is keep smaller than the cutoff in all the cases. Note, in particular, that the neutrino mean free path varies dramatically with the temperature, decreasing about two or three orders of magnitude when increasing the temperature from 5 to 50 MeV. Since the typical radius of a neutron star is of the order of 10–12 km, one can easily conclude from these results that a neutrino is unlikely to interact with matter at low temperatures. This conclusion is similar to those already derived by other authors. Our interest here, as we have said, is to analyze the convergence of the dynamical structure factor and the neutrino mean free path with the order of the power counting of the chiral forces, as well as their dependence on the cutoff employed.

Let us analyze first the effect of the cutoff of the chiral forces on the dynamical structure factor and the neutrino mean free path. In Fig. 3 we show the energy dependence of the dynamical structure factor $S(q_0, \vec{q}, T)$ evaluated at $T = 10$ MeV and $\rho = 0.16$ fm^{-3} using the chiral potential at LO [Fig. 3(a)], NLO [Fig. 3(b)], N^{2}LO [Fig. 3(c)], and N^{3}LO [Fig. 3(d)] for three values of the cutoff $\Lambda = 450$, 500, and 500 MeV. The density dependence of the neutrino mean free path for the same values of the cutoff and temperature is reported in Fig. 4. Note that whereas both $S(q_0, \vec{q}, T)$ and λ show a dependence on the cutoff Λ when the chiral potential is considered only at LO and NLO, this dependence is strongly reduced when higher-order contributions to the nuclear force are taken into account, being almost negligible at N^{3}LO. This reduction of

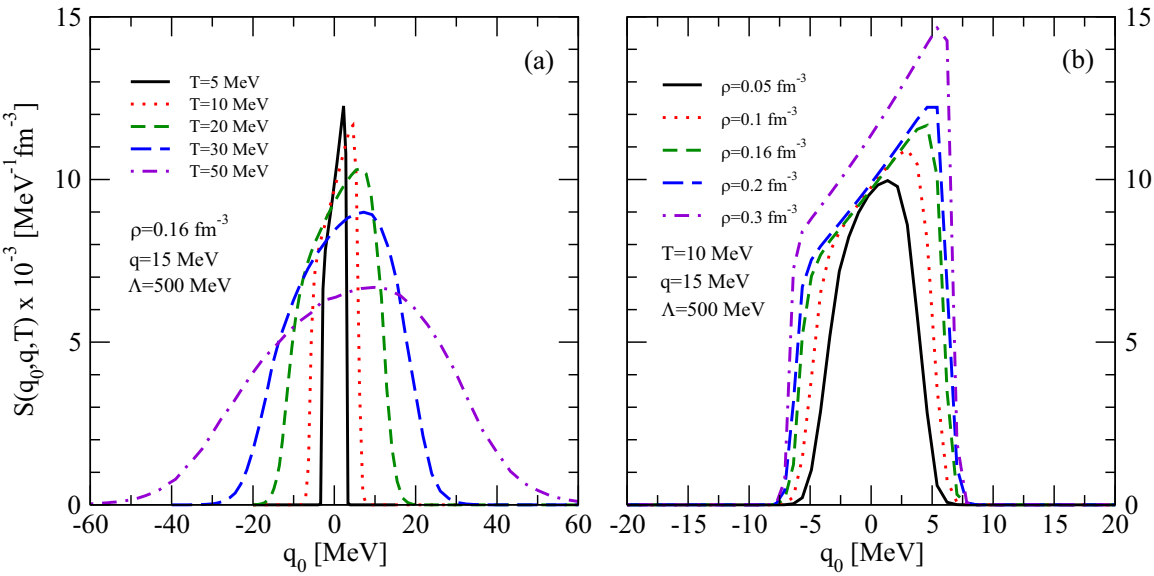

FIG. 1. Energy dependence of the dynamical structure factor $S(q_0, \vec{q}, T)$ for several temperatures at (a) a fixed density $\rho = 0.16$ fm^{-3} and (b) various densities at a fixed temperature $T = 10$ MeV. The calculation is done using the chiral potential at N^{3}LO including three-nucleon forces with a cutoff $\Lambda = 500$ MeV. The transferred three-momentum is taken as $|\vec{q}| = 15$ MeV.

the cutoff dependence is due to the effect of three-nucleon forces that start to contribute at N^{2}LO. This result is in agreement with the strong reduction of the cutoff dependence found for the energy per particle of neutron matter when including the contributions of three-body potentials (see, e.g., Ref. [100]). To illustrate it, in Figs. 4(c) and 4(d) we also show (see thin lines) the results when only the contribution of two-body forces is taken into account. As it can be seen, when the contribution of three-nucleon forces is ignored, the neutrino mean free path shows a considerable dependence on the cutoff still at N^{2}LO and N^{3}LO. We should note that to restore properly the cutoff independence of the neutron matter EoS and the neutrino mean free path is crucial to treat chiral

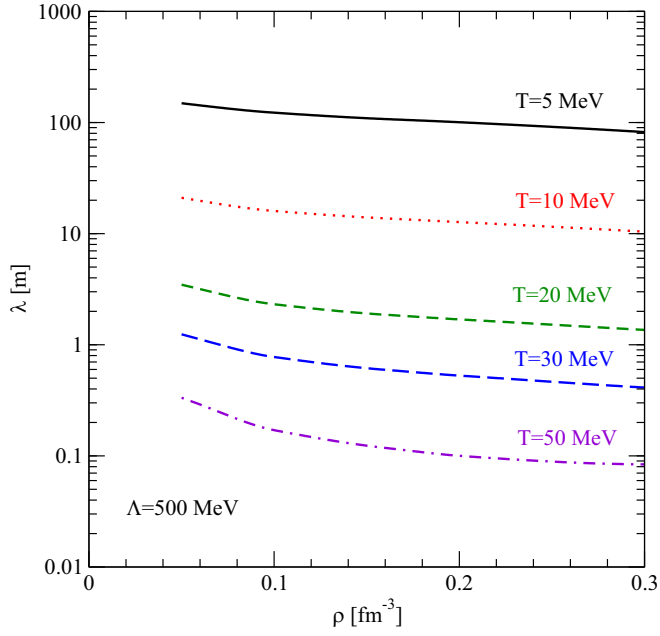

FIG. 2. Neutrino mean free path as a function of the baryon number density for temperatures in the range from 5 to 50 MeV. The calculation is done using the chiral potential at N^{3}LO including three-nucleon forces with a cutoff $\Lambda = 500$ MeV. The energy of the neutrino is assumed to be $E_\nu = 3T$.

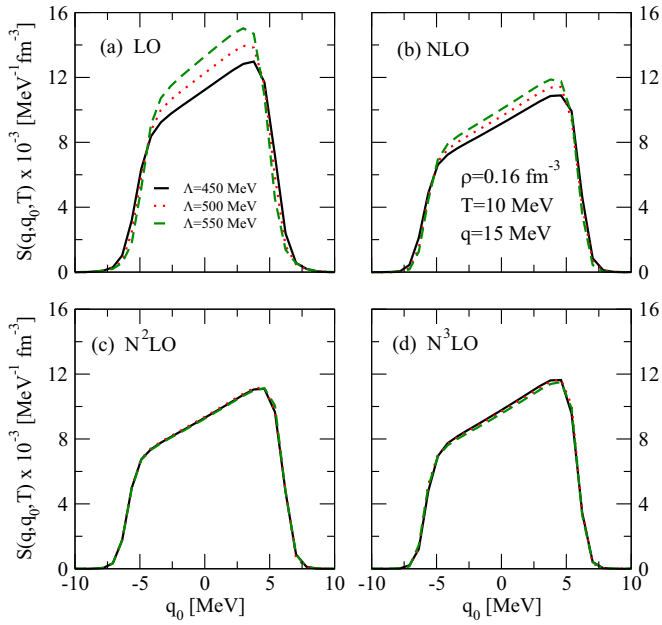

FIG. 3. Energy dependence of the dynamical structure factor $S(q_0, \vec{q}, T)$ for several values of the cutoff Λ at $T = 10$ MeV and $\rho = 0.16$ fm^{-3}. Results using the chiral potential at different orders are shown in the different panels. The transferred three-momentum is taken as $|\vec{q}| = 15$ MeV. The energy of the neutrino is assumed to be $E_\nu = 3T$.

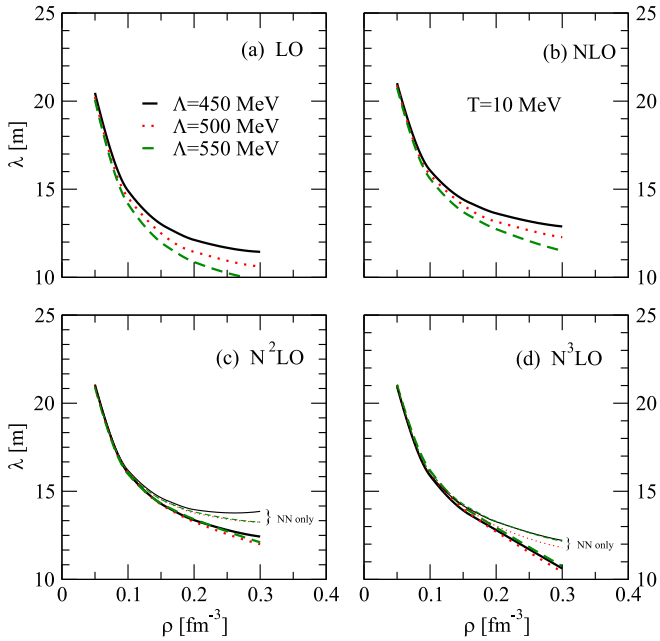

FIG. 4. Density dependence of the neutrino mean free path for several values of the cutoff Λ at $T = 10$ MeV. Results using the chiral potential at different orders are shown in the different panels. The energy of the neutrino is assumed to be $E_\nu = 3T$. Thin lines in (c) and (d) show the result when only the contribution of two-nucleon forces is taken into account in the calculation.

two- and three-nucleon forces consistently, that is when the same parameters are used for the same vertices that occur in all diagrams involved, as it is the case of the chiral forces employed in the present work.

Finally, we show in Fig. 5 the dependence of the neutrino mean free path on the order of power counting of the chiral forces for the three values of the cutoff considered in the whole range of densities explored at $T = 10$ MeV. As it is seen, the neutrino mean free path converges up to densities slightly below ≈ 0.15 fm^{-3} when increasing the order of the chiral power counting, with the convergence being better for the two larger values of the cutoff, $\Lambda = 500$ MeV and $\Lambda = 550$ MeV. No signal of convergence, however, seems to exist for densities above this value. The resulting lack of a convergence pattern at densities larger than ≈ 0.15 fm^{-3} gives, nonetheless, an estimation of the theoretical uncertainties associated with our order-by-order nuclear many-body calculation of the dynamical structure factor and the neutrino mean free path in hot neutron matter with chiral nuclear forces. As we showed before, the results at N^{2}LO and N^{3}LO are quite independent of the value of the cutoff Λ. Therefore, the variation obtained by changing Λ does not seem to provide a reliable representation of the uncertainty at a given order; a better way to estimate such uncertainty is to consider instead the difference between the predictions at two consecutive orders. The difference between results for the neutrino mean free path obtained using chiral nuclear forces at N^{2}LO and N^{3}LO at $T = 10$ MeV is shown in Table I for the three values of the cutoff considered and three representative densities, $\rho = 0.1$, 0.2, and 0.3 fm^{-3}. As it is seen, in general this difference is slightly smaller when a larger value of the cutoff is used, and it varies from about a few centimeters up to a bit less than 2 m in the whole range of densities considered.

TABLE I. Absolute value of the difference between the neutrino mean free path obtained using chiral nuclear forces at N^{2}LO and N^{3}LO at $T = 10$ MeV. Units are given in meters.

Density ρ (fm^{-3})	$\Lambda = 450$ MeV	$\Lambda = 500$ MeV	$\Lambda = 550$ MeV
0.1	0.16	0.07	0.19
0.2	0.57	0.55	0.48
0.3	1.81	1.57	1.35

IV. SUMMARY AND CONCLUSIONS

In this work we analyzed the role played by chiral nuclear forces on the propagation of neutrinos in hot neutron matter. In particular, we studied the convergence of the dynamical

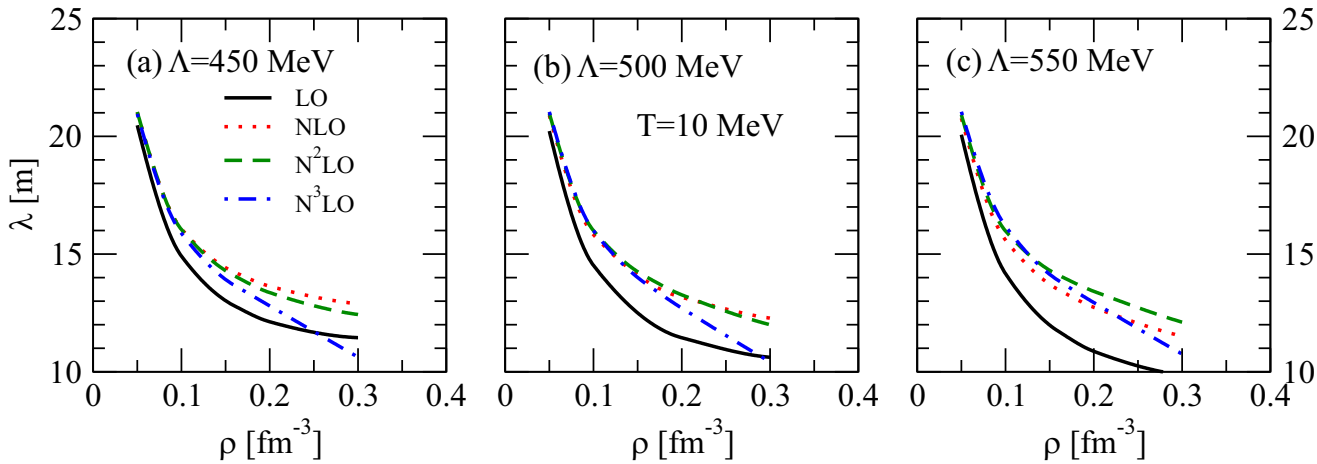

FIG. 5. Dependence of the neutrino mean free path on the order of power counting of the chiral forces for the three values of the cutoff considered in the whole range of densities explored at $T = 10$ MeV. The energy of the neutrino is assumed to be $E_\nu = 3T$.

structure factor and the neutrino mean free path when different orders in the chiral power counting are considered in the description of neutron matter, as well as the role of the regulator cutoff of these forces in the determination of these quantities. The dynamical structure factor and the neutrino mean free path were obtained using neutron single-particle energies and chemical potentials determined within the microscopic BHF approximation extended to finite temperature. We found that when the chiral force is considered at N^2LO the dependence of the dynamical structure factor and the neutrino mean free path on the cutoff is strongly reduced and becomes almost negligible at N^3LO, with the three-nucleon forces, that start to contribute at N^2LO, being responsible for the restoration of the cutoff independence. Finally, we found that the neutrino mean free path converges up to densities slightly below ≈ 0.15 fm^{-3} when increasing the order of the chiral power counting, although no signal of convergence is found for densities above this one. We roughly estimated the uncertainty associated with our order-by-order nuclear many-body calculation of the neutrino mean free path by evaluating the difference between the results obtained at N^2LO and N^3LO, finding that it varies from about a few centimeters at low densities up to a bit less than 2 m at the largest one considered in this work, 0.3 fm^{-3}. The extension of the present study to the case of hot asymmetric nuclear matter, more relevant to describe the physical conditions of newly born neutron stars, will be considered in the near future [72].

[1] D. L. Tubbs and D. N. Schram, Astrophys. J. **201**, 467 (1975).
[2] R. F. Sawyer, Phys. Rev. D **11**, 2740 (1975).
[3] D. Q. Lamb and C. J. Pethick, Astrophys. J. **209**, L77 (1976).
[4] D. Q. Lamb, J. M. Lattimer, C. J. Pethick, and D. G. Ravenhall, Phys. Rev. Lett. **41**, 1623 (1978).
[5] D. L. Tubbs, Astrophys. J. Suppl. Series **37**, 287 (1978).
[6] S. Bludman and K. Van Riper, Astrophys. J. **224**, 631 (1978).
[7] R. F. Sawyer and A. Soni, Astrophys. J. **230**, 859 (1979).
[8] N. Iwamoto, Ann. Phys. **141**, 1 (1982).
[9] N. Iwamoto and C. J. Pethick, Phys. Rev. D **25**, 313 (1982).
[10] B. T. Goodwin and C. J. Pethick, Astrophys. J. **253**, 816 (1982).
[11] A. Burrows and T. J. Mazurek, Astrophys. J. **259**, 330 (1982).
[12] B. T. Goodwin, Astrophys. J. **261**, 321 (1982).
[13] S. W. Bruenn, Astrophys. J. Suppl. Series **58**, 771 (1985).
[14] L. J. van den Horn and J. Cooperstein, Astrophys. J. **300**, 142 (1986).
[15] O. V. Maxwell, Astrophys. J. **316**, 691 (1987).
[16] J. Cooperstein, Phys. Rep. **163**, 95 (1988).
[17] A. Burrows, Astrophys. J. **334**, 891 (1988).
[18] R. F. Sawyer, Phys. Rev. C **40**, 865 (1989).
[19] P. J. Schinder, Astrophys. J. Suppl. Series **74**, 249 (1990).
[20] C. J. Horowitz and K. Wehrberger, Nucl. Phys. A **531**, 665 (1991).
[21] C. J. Horowitz and K. Wehrberger, Phys. Rev. Lett. **66**, 272 (1991).
[22] C. J. Horowitz and K. Wehrberger, Phys. Lett. B **266**, 236 (1991).
[23] M. Prakash, M. Prakash, J. Lattimer, and C. J. Pethick, Astrophys. J. **390**, L77 (1992).
[24] S. Reddy and M. Prakash, in *Advances in Nuclear Dynamics*, edited by W. Bauer and A. Mignerey (Plenum, New York, 1995), pp. 237–245.
[25] W. Keil, H.-Thomas Janka, and G. Raffelt, Phys. Rev. D **51**, 6635 (1995).
[26] H.-T. Janka, W. Keil, G. Raffelt, and D. Seckel, Phys. Rev. Lett. **76**, 2621 (1996).
[27] G. Sigl, Phys. Rev. Lett. **76**, 2625 (1996).
[28] S. Reddy and M. Prakash, Astrophys. J. **478**, 689 (1997).
[29] S. Reddy, M. Prakash, and J. M. Lattimer, Phys. Rev. D **58**, 013009 (1998).
[30] S. Reddy, M. Prakash, J. M. Lattimer, and J. A. Pons, Phys. Rev. C **59**, 2888 (1999).
[31] J. Navarro, E. S. Hernández, and D. Vautherin, Phys. Rev. C **60**, 045801 (1999).
[32] S. Reddy, G. Bertsch, and M. Prakash, Phys. Lett. B **475**, 1 (2000).
[33] M. Prakash, J. M. Lattimer, R. F. Sawyer, and R. R. Volkas, Annu. Rev. Nucl. Part. Sci. **51**, 295 (2001).
[34] J. Margueron, J. Navarro, and B. Van Giai, Nucl. Phys. A **719**, C169 (2003).
[35] J. Margueron, I. Vidaña, and I. Bombaci, Phys. Rev. C **68**, 055806 (2003).
[36] C. Shen, U. Lombardo, N. Van Giai, and W. Zuo, Phys. Rev. C **68**, 055802 (2003).
[37] C. J. Horowitz, M. A. Pérez-García, and J. Piekarewicz, Phys. Rev. C **69**, 045804 (2004).
[38] A. Burrows, S. Reddy, and T. A. Thompson, Nucl. Phys. A **777**, 356 (2006).
[39] J. Margueron, N. Van Giai, and J. Navarro, Phys. Rev. C **74**, 015805 (2006).
[40] P. Gögelein and H. Müther, Phys. Rev. C **76**, 024312 (2007).
[41] P. Grygorov, P. Gögelein, and H. Müther, J. Phys. G: Nucl. Part. Phys. **37**, 075203 (2010).
[42] L. F. Roberts, S. Reddy, and G. Shen, Phys. Rev. C **86**, 065803 (2012).
[43] C. J. Horowitz, G. Shen, E. O'Connor, and C. D. Ott, Phys. Rev. C **86**, 065806 (2012).
[44] G. Martínez-Pinedo, T. Fischer, A. Lohs, and L. Huther, Phys. Rev. Lett. **109**, 251104 (2012).
[45] G. Shen and S. Reddy, Phys. Rev. C **89**, 032802(R) (2014).
[46] E. Rrapaj, J. W. Holt, A. Bartl, S. Reddy, and A. Schwenk, Phys. Rev. C **91**, 035806 (2015).
[47] L. F. Roberts and S. Reddy, Phys. Rev. C **95**, 045807 (2017).
[48] J. Torres Patiño, E. Bauer and I. Vidaña, Phys. Rev. C **99**, 045808 (2019).
[49] E. Bauer and J. Torres Patiño, Phys. Rev. C **101**, 065806 (2020).
[50] M. Oertel, A. Pascal, M. Mancini, and J. Novak, Phys. Rev. C **102**, 035802 (2020).
[51] H. A. Bethe, Rev. Mod. Phys. **62**, 801 (1990).
[52] Th. Janka and E. Müller, Astron. Astrophys. **306**, 167 (1996).
[53] A. Burrows, Nature (London) **403**, 727 (2000).

[54] A. Burrows and J. M. Lattimer, Astrophys. J. **307**, 178 (1986).
[55] H.-T. Janka and E. Muller, Astrophys. J. Lett. **448**, L109 (1995).
[56] I. Bombaci, Astron. Astrophys. **305**, 871 (1996).
[57] M. Prakash, I. Bombaci, M. Prakash, P. J. Ellis, J. M. Lattimer, and R. Knorren, Phys. Rep. **280**, 1 (1997).
[58] I. Vidaña, I. Bombaci, A. Polls, and A. Ramos, Astron. Astrophys. **399**, 687 (2003).
[59] G. F. Burgio, H.-J. Schulze, and A. Li, Phys. Rev. C **83**, 025804 (2011).
[60] A. Perego, S. Rosswog, R. Cabezón, O. Korobkin, R. Kaeppeli, A. Arcones, and M. Liebendoerfer, Mon. Not. R. Astron. Soc. **443**, 3134 (2014).
[61] D. Martin, A. Perego, A. Arcones, F.-K. Thielemann, O. Korobkin, and S. Rosswog, Astrophys. J. **813**, 2 (2015).
[62] M. Frensel, M.-R. Wu, C. Volpe, and A. Perego, Phys. Rev. D **95**, 023011 (2017).
[63] M. Cusinato, F. M. Guercilena, A. Perego, D. Logoteta, D. Radice, S. Bernuzzi, and S. Ansoldi, Eur. Phys. J. A **58**, 99 (2022).
[64] D. Radice, S. Bernuzzi, A. Perego, and R. Hass, Mon. Not. R. Astron. Soc. **512**, 1499 (2022).
[65] Y. A. Shibanov and D. G. Yakovlev, Astron. Astrophys. **309**, 171 (1996).
[66] D. G. Yakovlev, A. D. Kaminker, O. Y. Gnedin, and P. Haensel, Phys. Rep. **354**, 1 (2001).
[67] D. G. Yakovlev and C. J. Pethick, Annu. Rev. Astron. Astrophys. **42**, 169 (2004).
[68] Z. Lin and C. J. Horowitz, Phys. Rev. C **96**, 055804 (2017).
[69] T. Fischer, G. Guo, A. A. Dzhioev, G. Martínez-Pinedo, M.-R. Wu, A. Lohs, and Y.-Z. Qian, Phys. Rev. C **101**, 025804 (2020).
[70] B. Fore and S. Reddy, Phys. Rev. C **101**, 035809 (2020).
[71] G. Guo, G. Martínez-Pinedo, A. Lohs, and T. Fischer, Phys. Rev. D **102**, 023037 (2020).
[72] I. Vidaña, D. Logoteta and I. Bombaci (unpublished).
[73] I. Tews, T. Krüger, K. Hebeler, and A. Schwenk, Phys. Rev. Lett. **110**, 032504 (2013).
[74] A. Carbone, A. Polls, and A. Rios, Phys. Rev. C **88**, 044302 (2013).
[75] A. Carbone, A. Rios, and A. Polls, Phys. Rev. C **90**, 054322 (2014).
[76] K. Hebeler, J. D. Holt, J. Menendez, and A. Schwenk, Annu. Rev. Nucl. Part. Sci. **65**, 457 (2015).
[77] I. Tews, S. Gandolfi, A. Gezerlis, and A. Schwenk, Phys. Rev. C **93**, 024305 (2016).
[78] C. Drischler, A. Carbone, K. Hebeler, and A. Schwenk, Phys. Rev. C **94**, 054307 (2016).
[79] J. W. Holt and N. Kaiser, Phys. Rev. C **95**, 034326 (2017).
[80] I. Bombaci and D. Logoteta, Astron. Astrophys. **609**, A128 (2018).
[81] C. Drischler, K. Hebeler, and A. Schwenk, Phys. Rev. Lett. **122**, 042501 (2019).
[82] M. Piarulli, I. Bombaci, D. Logoteta, A. Lovato, and R. B. Wiringa, Phys. Rev. C **101**, 045801 (2020).
[83] D. Logoteta, A. Perego, and I. Bombaci, Astron. Astrophys. **646**, A55 (2020).
[84] C. Drischler, J. W. Holt, and C. Wellenhofer, Annu. Rev. Nucl. Part. Sci. **71**, 403 (2021).
[85] F. Sammarruca and R. Millerson, Phys. Rev. C **104**, 034308 (2021).
[86] J. Keller, C. Wellenhofer, K. Hebeler, and A. Schwenk, Phys. Rev. C **103**, 055806 (2021).
[87] A. Lovato, I. Bombaci, D. Logoteta, M. Piarulli, and R. B. Wiringa, Phys. Rev. C **105**, 055808 (2022).
[88] S. Bacca, K. Hally, C. J. Pethick, and A. Schwenk, Phys. Rev. C **80**, 032802(R) (2009).
[89] S. Bacca, M. Liebendörfer, A. Perego, C. J. Pethick, and A. Schwenk, Astrophys. J. **758**, 34 (2012).
[90] G. Guo and G. Martínez-Pinedo, Astrophys. J. **887**, 58 (2019).
[91] L. Riz, F. Pederiva, and S. Gandolfi, J. Phys. G: Nucl. Part. Phys. **47**, 045106 (2020).
[92] C. J. Joachin, *Quantum Collision Theory* (North-Holland, Amsterdam, 1975).
[93] P. Chomaz, D. Vautherin, and N. Vinh Mau, Phys. Lett. B **242**, 313 (1990).
[94] D. R. Entem, R. Machleidt, and Y. Nosyk, Phys. Rev. C **96**, 024004 (2017).
[95] E. Epelbaum, A. Nogga, W. Glöckle, H. Kamada, Ulf-G. Meißner, and H. Witala, Phys. Rev. C **66**, 064001 (2002).
[96] V. Bernard, E. Epelbaum, H. Krebs, and Ulf-G. Meißner, Phys. Rev. C **77**, 064004 (2008).
[97] J. W. Holt, N. Kaiser, and W. Weise, Phys. Rev. C **79**, 054331 (2009).
[98] N. Kaiser and B. Singh, Phys. Rev. C **100**, 014002 (2019).
[99] N. Kaiser, arXiv:2010.02739.
[100] L. Coraggio, J. W. Holt, N. Itaco, R. Machleidt, and F. Sammarruca, Phys. Rev. C **87**, 014322 (2013).